Ion Atmosphere of Three-Way Junction Nucleic Acid†

Udayan Mohanty,*,‡,§ Alexander Spasic,‡ Harold D. Kim,§ and Steven Chu§

Department of Chemistry, Boston College, Chestnut Hill, Massachusetts 02467, and Department of Physics and Applied Physics, Stanford University, Stanford, California 94305-4060

Received: January 1, 2005; In Final Form: March 24, 2005

The ion atmosphere of three-armed symmetric Y-shaped and asymmetric y-shaped A−RNA junctions in aqueous solution containing multivalent ions is described within the framework of a polyelectrolyte model. The fraction of "screening counterions" per polyion charge that shield the residual unneutralized charges from interacting with one another and the condensed counterions per polyion charge as a function of sodium and magnesium ion concentrations are determined. The predictions for the slope of $\log(k_o/k_f)$ as a function of Na^+ and Mg^{2+} concentration, where k_o and k_f are the opening and folding rates of the three-helix junction molecule, respectively, are compared with experimental data (Kim et al. *Proc. Nat. Acad. Sci. U.S.A.* **2002**, *96*, 9077−9082).

Structural motifs such as pseudoknots and helical junctions are fundamental building blocks of global RNA structure. The establishment of these building blocks provides the initial step in the folding pathways of the macromolecule.[1] Nucleic acid junction elements share certain characteristics in common such as coaxial stacking of helices and interaction with multivalent cations.[2,3] The significance of these canonical features is typified in the hammerhead ribozyme. The eleven nucleotides at the junction of the Y-shaped three-way helical stems are critical for catalytic activity.[4] The ribozyme cleaves a substrate RNA in the presence of magnesium cofactor.[5] Furthermore, polyacrylamide gel electrophoresis (PAGE) reveals that the three helices of the ribozyme change conformations in the presence of added multivalent cations.[6]

Stability of RNAs in aqueous solution is governed by the interplay of nonelectrostatic and electrostatic forces that act on them.[7,8,9] It is generally regarded that counterions interact with the backbone of RNA by long-range Coulombic interactions, and that these interactions are nonspecific in nature.[8] These counterions are "condensed" but form a "delocalized" cloud that screens the repulsive phosphate−phosphate interactions along the backbone of the polyion.[8] In contrast, site binding takes into account the hydration state of the ion.[9] In "outer-sphere" binding, cations are trapped in pockets of negative electrostatic potential in the proximity of the surface of a nucleic acid.[9,10,11] A basic feature of an "inner-sphere" binding is that the cations are in contact with the RNA ligand without overlap of their solvation shells.[9,10,12] In fact, crystal structures of the P4−P6 domain of *Tetrahymena* group I intron[13] and hammerhead ribozyme[14] reveal the presence of specific ion−RNA complexes. Even though there has been considerable progress toward describing how magnesium cations interact with RNA, the ultimate distinction between site and diffuse binding must reside in the energetics of such processes in solution.[9,10]

In the absence of magnesium ions, *Bacillus stearothermophilus* ribosomal protein S15 interacts with the conserved three-way junction located in the central domain of eubacterial 16S rRNA[15] and leads to significant conformational changes in helices 20, 21, and 22 such that there is coaxial stacking between helices 21 and 22, with helix 20 making an angle of 60° with helix 22.[3,15,16] It is unclear, however, whether protein S15 fixes a configuration that is accessed via natural fluctuation or whether it induces a conformational change. In the unfolded form, the angles between helices 20, 21, and 22 are approximately equal (120°). This junction can also be folded by magnesium cations.[3,16] In fact, current experimental evidence indicates that the conformation induced by magnesium is rather similar to that induced by S15.[3] Three out of the eight Mg^{2+} ions observed crystallographically are essential for the stabilization of the junction formed from the S15−rRNA complex.[17] Magnesium ions are generally believed to enhance the rate of association of the protein with the binding site of RNA by a shift of the equilibrium between the unfolded and folded states of the junction.[3,15,16]

In a recent work, Kim et al.[18] have exploited single-molecule fluorescence energy transfer (FRET)[19,20] and fluorescence correlation spectroscopy (FCS)[21,22] to probe the conformational changes of the three-helix junction in the central domain of 16S ribosomal RNA. In the experiment, the three-helix junction was immobilized on a glass surface by attaching a biotin moiety to one of the arms.[18] A Cy3-Cy5 donor−acceptor pair was attached to the remaining two ends of the helical junction.[10] Several noteworthy results were obtained. First, fluorescence fluctuations between two FRET states occurred on a millisecond time scale.[18] Second, the transition between the two conformations was dependent on both sodium and magnesium ion concentrations.[10] Third, the folding and opening rates of the helical junction, denoted by k_f and k_o, respectively, were dependent on salt concentration.[18] In fact, both Na^+ and Mg^{2+} ions speed up the folding rate of the unfolded junction, while they reduce the unfolding rate of the folded state.[18]

In this work, a polyelectrolyte model describes the characteristics of the ion atmosphere in the proximity of Y-shaped and asymmetric y-shaped A−RNA junctions. The predictions for the dependence of opening and folding rates of the RNA three-way structural element on Mg^{2+} and Na^+ concentrations are compared with single-molecule FCS and FRET data of Kim et al.[18]

† Part of the special issue "Irwin Oppenheim Festschrift".
‡ Boston College.
§ Stanford University.

10.1021/jp050005o CCC: $30.25
Published on Web 05/12/2005

Theoretical Methods

Counterions Atmosphere. When polyelectrolytes such as RNA and DNA are immersed in an ionic solvent, counterions from the bulk solution will condense and form a delocalized cloud that shields the negative phosphate charges. This phenomenon of counterion condensation is governed by the dimensionless linear charge density parameter ξ defined as the ratio of two length scales, namely the Bjerrum length l_B and the axial charge spacing b along the backbone of the nucleic acid.[8,23] The Bjerrum length is the characteristic distance at which the Coulomb energy between a pair of charges balances thermal fluctuations at temperature T. For B−DNA and single-stranded DNA, the linear charge density ξ is 4.2 and 1.8, respectively.[8] Because ξ is larger than unity in RNA, the system is electrostatically unstable.[8,23] In fact, there is a critical charge density $\xi > 1/z_C$, where z_C is the valence of the counterion, that signals the onset of counterion condensation. Under this condition, counterion condensation takes place so as to reduce the effective charge of the polyion. In the limiting law condition (i.e., low salt), θ, the number of condensed counterions per polyion charge, is given by[8]

$$z_C\theta = 1 - \frac{1}{z_C\xi} \tag{1}$$

Each phosphate charge is reduced by an amount $1 - z_C\theta$ due to the condensed counterions.

Consider a ligand L of charge $+z$ that binds to a polyelectrolyte P such as RNA. To describe this phenomenon, a binding equilibrium of the generic form needs to be considered

$$L + P \underset{k_o}{\overset{k_f}{\rightleftharpoons}} LP$$

where k_f and k_o are the forward and the reverse rate constants. The thermodynamic equilibrium constant $K_{eq} = K_{obs}{\cdot}K_\gamma$, where K_{obs} is the equilibrium ratio of the concentration of products and reactants, [LP]/([P][L]), and K_γ is the corresponding ratio of the activity coefficients (i.e., coefficients that incorporate deviations of the system from ideality).[7] Thermodynamic arguments based on the counterion condensation model suggest that the salt dependence of the intrinsic binding constant (i.e., that obtained by extrapolation to zero density) satisfies[7,8]

$$\frac{\partial \log K_{obs}}{\partial \log [M^+]} = -z \tag{2}$$

where $[M^+]$ is the concentration of cations in aqueous solution. Observe that the right-hand side of eq 2 is independent of the conformation of the polyelectrolyte. Thus, when the charged ligand of valence z binds to a nucleic acid, it neutralizes z phosphate charges that result in the release of counterions that have been associated with the phosphates.

In aqueous solution, polyion−ion interaction leads to the accumulation of counterions and the exclusion of coions around a nucleic acid. To elucidate the role played by the inhomogeneous distribution of salt ions, it is fruitful to introduce the concept of preferential interaction coefficient Γ.[7,24] The importance of preferential interaction coefficient stems from the fact that it describes the nonideality between a polyelectrolyte and the electrolyte solution due to short-range repulsive as well as long-range Coulombic interactions.[7,24] The thermodynamic argument for a three-component system under the conditions of constant temperature and pressure leads to an approximate expression for the preferential interaction coefficient between the polyelectrolyte, P, in a solvent generally taken to be water and an electrolyte component, s,[7]

$$-\left(\frac{\partial \ln K_{obs}}{\partial \ln c_s}\right)_{c_P \to 0} = (1 + 2\Gamma_{sP}) \tag{3}$$

Here, c_s is the salt concentration, c_P is the concentration of the polyelectrolyte, and $(1 + 2\Gamma_{sP})$ is the difference in counterion association of the products and the reactants. If $(1 + 2\Gamma_{sP})$ is negative, then the process of converting reactants to products will lead to the release of thermodynamically associated counterions.[7]

Binding of Counterions. A quantitative prediction of the salt dependence of the intrinsic binding constant for three-way junctions requires a model for the fraction of the charge neutralized by the condensed counterions, θ, that is valid at both low and high salt concentrations. Because the low salt ion atmosphere around a nucleic acid is described well by counterion condensation,[8] we consider a model that is capable of describing the ion atmosphere of nucleic acid under moderately high salt condition.

Let the polyion (P) have N charges, each of magnitude q. Let the valence of the counterions (C) be $|z_c|$. Assume that there is one counterion binding site per polyion charge. Let n_C denote the number of counterions that bind to the polyion to produce a complex, labeled D(J, n_C), in configuration J: $n_C C + P \rightleftharpoons D(J, n_C)$. The equilibrium condition for the reaction is

$$n_C\mu_C + \mu_P \rightleftharpoons \mu_{D(J,n_C)} \tag{4}$$

where μ denotes the chemical potential of the species under consideration. The chemical potential of the jth species is approximately

$$\mu_j \approx \mu_j^o + k_B T \ln\left(\frac{m_j}{m_o}\right) \tag{5}$$

where m_o is the molarity of the solvent (water), m_j is the molarity of species j, μ_j^o is the standard chemical potential of species j, k_B is the Boltzmann constant, and T is the absolute temperature.

It is fruitful to partition the standard-state chemical potentials between the various species as[25]

$$\mu^o_{D(J,n_C)} - \mu^o_P - n_C\mu^o_C = A_{elec}(J, n_C) - A_{elec}(0) + n_C\Delta A_{transf} \tag{6}$$

where $A_{elec}(J, n_C)$ and $A_{elec}(0)$ are the electrostatic free energy of the various subunits of the complex due to long-range electrostatic interactions and the bare polyion respectively, while ΔA_{transf} is the free energy due to transfer of a counterion from the bulk to the binding site. By making use of eqs 4−6, one obtains[25]

$$\frac{m_D}{m_P} \equiv \sum_{n_C}^{N}\sum_{J}\frac{m_{D(J,n_C)}}{m_P} = \sum_{n_C=1}^{N}\left(\frac{m_C\chi}{m_o}\right)^{n_C}\sum_{J}\exp[-[A_{elec}(J, n_C) - A_{elec}(0)]/k_BT] \tag{7}$$

where m_D and m_C are the total concentrations of complexes and counterions, respectively, and $\chi = \exp(-\Delta A_{transf}/k_BT)$. The distribution of counterions along the backbone of an ionic

oligomer is uniform except near its ends.[7,23b] To proceed further, assume that the dominant contribution in the sum over J is that configuration $\bar{J}$ for which the condensed counterions are distributed uniformly.[25] Partition the binding sites of the polyion into n_C domains. Each domain has (N/n_C) binding sites. In a uniform distribution, there is one counterion in a domain. Thus, the number of uniform configurations is approximately $(N/n_C)^{n_C}$, and eq 7 simplifies to[25]

$$\frac{m_D}{m_P} \approx \sum_{n_C=1}^{N} \left(\frac{m_C\chi}{m_o}\right)^{n_C} \exp[-[A_{elec}(n_C) - A_{elec}(0)]/k_BT](N/n_C)^{n_C} \quad (8)$$

The above expression is evaluated by maximum term methodology. The maximum term occurs at, say, $n_C = \bar{n}_C$ and satisfies the condition[25]

$$\frac{\partial}{\partial \bar{n}_C}\left\{\bar{n}_C \ln\left(\frac{m_C\chi}{m_o}\right) - [A_{elec}(\bar{n}_C) - A_{elec}(0)]/k_BT + \bar{n}_C \ln(N/\bar{n}_C)\right\} = 0 \quad (9)$$

Solving for $\bar{n}_C$, we find the fraction of condensed counterions per polyion charge

$$\theta = \frac{\bar{n}_C|z_C|}{N} = m_C(\chi/em_o)|z_C| \exp\left[-\frac{\partial(A_{elec}/k_BT)}{\partial \bar{n}_C}\right] \quad (10)$$

We assume that the charges on the polyion interact via screened Debye−Hückle potential.[8,26] In this case, the electrostatic free energy is[8,26]

$$A_{elec}(\bar{n}_C) = k_BT(1-\theta)^2 l_B N\, \Gamma(j,\kappa) \quad (11)$$

where l_B is the Bjerrum length, κ^{-1} is the Debye screening length and is related to the square root of the ionic strength I of the aqueous solution defined as $I = (^1/_2)m_C(z_C^2 + |z_C/z_d|z_d^2)$, where z_d is the valence of the coion. The quantity $\Gamma(j,\kappa)$ appearing in the electrostatic free energy is defined as

$$\Gamma(j,\kappa) = (^1/_2)\sum_{l\neq j} e^{-r_{jl}/\kappa} \quad (12)$$

Equations 10−12 lead to a nonlinear relation for θ, the fraction of condensed counterions per polyion charge in the ion atmosphere of the nucleic acid[25]

$$\theta = m_C(\chi/em_o)|z_C|e^{-1+2(1-\theta)l_B|z_C|\Gamma(j,\kappa)} \quad (13)$$

Note that θ is explicitly salt-dependent. Under limiting law conditions, however, eq 13 reduces to that given by counterion condensation formalism,[8] namely, eq 1.

Results and Discussion

RNA Junction Constructs. To examine the ion atmosphere and the accumulation of counterions around the three-helix junction studied by Kim et al.,[18] we have constructed a simplified model that mimics the shape and size of the junction. A threefold symmetric Y-shaped junction in which the arms connect to points that define an equilateral triangle as well as an asymmetric y-shaped junction in which the interarm angles are 60°, 120°, and 180° (Figure 1) were studied. The axial charge spacing (i.e., the separation of the negative phosphate charges) is taken to be 2.6 Å, a value appropriate for A−RNA.[8,26,27] The length of each arm of the three-way junction is taken to be 20 bp.

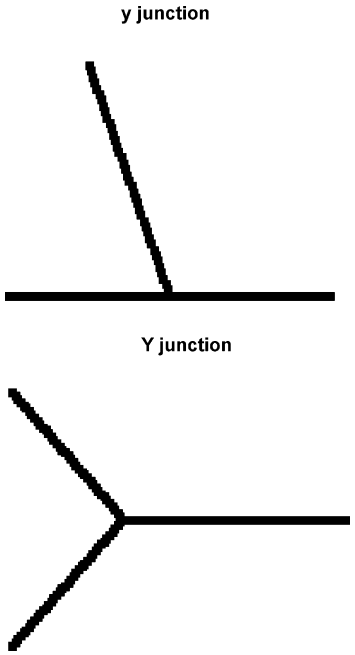

Figure 1. The figure schematically depicts RNA three-way junctions investigated in this work. In a threefold symmetric Y-shaped junction, the arms connect to points that define an equilateral triangle. In contrast, a y-shaped junction is defined as an asymmetric junction in which the interarm angles are 60°, 120°, and 180°.

Comparison with Experimental Data. The fraction of condensed counterions per polyion charge, θ, computed from the model is plotted in Figure 2 as a function of the logarithm of sodium ion concentration for threefold symmetric Y-shaped and asymmetric y-shaped A−RNA junction molecules. Several comments are in order. First, the buffer used in the experimental study consists of 10 mM Tris and 50 mM NaCl at pH = 8.[18] Because 100−1000 mM NaCl(aq) was added to the buffer,[18] the ionic strength varied between 170 and 1070 mM. Furthermore, 20−400 μM $MgCl_2$(aq) was also added to the buffer. With added magnesium concentration only, the ionic strength varied between 70.004 and 70.8 mM. Second, the range of salt concentrations in Figure 2 is the same as that utilized by Kim et al.[18] Third, the fractions of condensed counterions per polyion charge for both RNA junctions exhibit notable variation with $[Na^+]$. The number of associated counterions depends on the conformation of the junction. In the entire range of Mg^{2+} and Na^+ cations investigated, the number of associated counterions is largest for the asymmetric y-shaped A−RNA junction, while it is smallest for the linear A−RNA molecule, the reference molecule, whose length is equal to the total length of the three arms of the junction. Fourth, for comparative purpose, we have tabulated the number of associated counterions in the counterion condensation model in Table 1 and Table 2. Finally, for salt concentrations between 100 and 600 mM, the average value of θ is approximately 0.54 and 0.56 for symmetric Y-shaped and asymmetric y-shaped RNA junctions, respectively.

Figure 3 shows the radial distribution function $g(r)$ of counterion−RNA and coion−RNA within the framework of counterion condensation formalism[28] at 70 mM, the ionic strength of the buffer. A noteworthy feature is the existence of

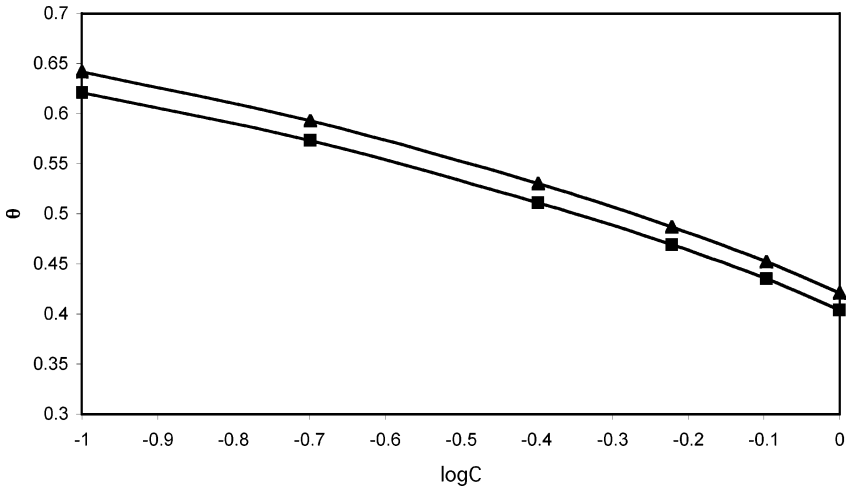

Figure 2. The fraction of condensed counterions, θ, per polyion charge as a function of log C, where $C = [Na^+]$ is the sodium ion concentration, for Y-shaped (square) and asymmetric y-shaped (triangle) RNA three-way junction molecules. The predictions are based on the model described in the text.

TABLE 1: Total Number of Associated Counterions for Various Conformations of Three-Way Junctions as a Function of Mg^{2+} Cation Concentration in the Manning Counterion Condensation Model[a]

Mg (μM)	linear	y-shape	Y-shape
20.00	95.40	98.04	97.32
60.00	96.24	98.88	98.16
120.0	96.96	99.60	98.88
160.0	97.44	99.96	99.24
240.0	98.16	100.44	99.96

[a]The second column is for a linear A−RNA molecule whose length is equal to the total length of the three arms of the junction.

TABLE 2: Total Number of Associated Counterions for Various Conformations of Three-Armed Junctions as a Function of Na^+ Cation Concentration in the Manning Counterion Condensation Model[a]

Na (mM)	linear	y-shape	Y -shape
100.0	94.56	96.48	96.00
200.0	96.36	97.92	97.44
400.0	98.04	99.24	98.88
600.0	99.12	100.08	99.84

[a]The second column is for a linear A−RNA molecule whose length is equal to the total length of the three arms of the junction.

three populations of ions around three-way junctions: a compact condensed layer of counterions located "near" the polyion surface, a "far away" diffuse Debye−Hückel counterion cloud that occurs at a distance from the polyion surface that equals the Debye screening length, and a cloud of coions (Cl^-) just outside ("intermediate" region) the condensed layer. The cloud of coions and the Debye−Hückle counterions, termed the "screening counterions", shield the residual unneutralized charges from interacting with one another.[7,8]

The fraction of screening counterions per polyion charge is

$$\psi_s = 1/(2\xi) \tag{14}$$

where ξ is the Manning linear charge density. Equation 14 is derived in a straightforward fashion from the activity coefficient γ of the polyelectrolyte solution that is given by $\gamma \approx (\kappa b)^{-N/\xi}$.[8,29] For A−RNA, the fraction of "screening counterions" per polyion charge is $\psi_s = 0.18$. Therefore, the total fraction of bound counterions is 0.72 and 0.74 for symmetric Y-shaped and asymmetric y-shaped A−RNA junctions, respectively.

How does the above prediction compare with the single-molecule FRET and FCS experimental data of Kim et al.?[18] What has been measured experimentally is the dependence of the observed opening and folding rates of the three-helix junction, k_o and k_f, respectively, on $[Na^+]$. We have plotted in Figure 4, $\log(k_o/k_f)$, obtained from the experimental data of Kim et al.,[18] as function of $-\log[Na^+]$. A notable feature of the data is that the variation of the observed equilibrium constant over

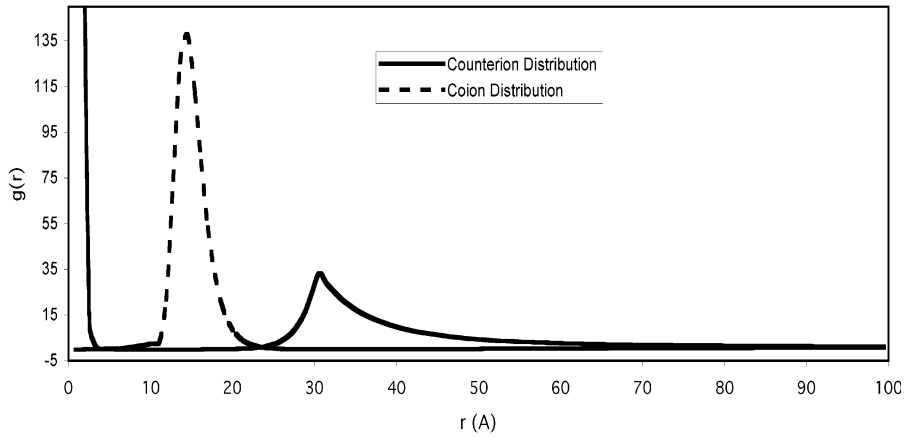

Figure 3. The radial distribution functions $g(r)$ for counterion−RNA (continuous line) and for coion−RNA (dashed line) as a function of radial distance r from the surface of the polyion at 70 mM salt concentration. Observe the existence of three populations of ions in the vicinity of the macromolecule.

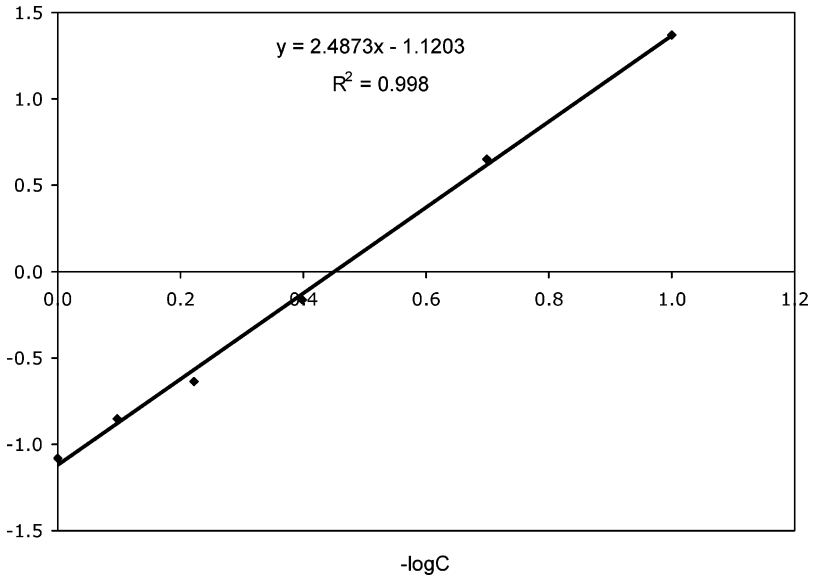

Figure 4. The figure is a plot of log K as a function of $-\log C$. Here, $C = [Na^+]$ is the concentration of sodium ion added to the buffer, and $K = k_o/k_f = K_{obs}$ where k_o and k_f are the experimental opening and folding rates of the RNA three-helix junction obtained from ref 18. The equation of the straight line (black line) that is a best fit to the experimental data (square) and the corresponding R^2 value are shown as an inset in the figure.

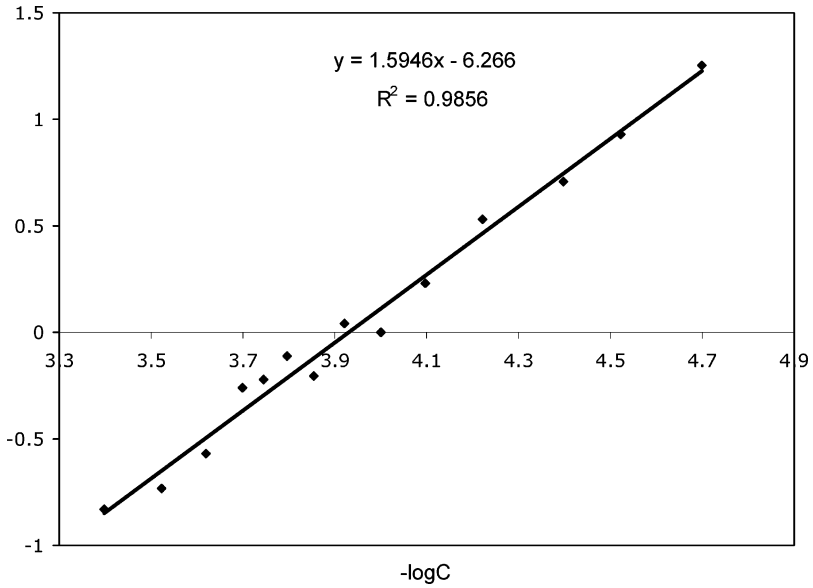

Figure 5. The figure is a plot of log K as a function of $-\log C$. Here, $C = [Mg^{2+}]$ is the concentration of magnesium ion added to the buffer, and $K = k_o/k_f = K_{obs}$ where k_o and k_f are the experimental opening and folding rates of the RNA three-helix junction obtained from ref 18. The equation of the straight line (black line) that is a best fit to the experimental data (square) and the corresponding R^2 value are shown as an inset in the figure.

the range of sodium ion concentration between 100 and 600 mM is

$$-\frac{\partial \log K_{obs}}{\partial \log[Na^+]} \approx 2.59 \qquad (15)$$

The right hand side of eq 15 is $n_{eff}(\theta + \psi_s)$, where n_{eff} is the number of ion pairs that is formed.[7] The sum of θ and ψ_s is 0.72 and 0.74 for symmetric Y-shaped and asymmetric y-shaped, respectively. Hence, n_{eff} is approximately 3.5. This value for n_{eff} agrees with the Hill coefficient obtained by Kim et al.[18]

A quantitative description of how $[Mg^{2+}]$ influences the folding and opening rates of three-helix RNA junction is based on the following observations. First, the buffer has 50 mM NaCl-(aq).[18] Second, what is varied in the experiment is the concentration of Mg^{2+} ions in the micromolar range at fixed T and P and excess Na^+ ions.[18] Third, under these conditions, the fraction of divalent counterions per polyion charge is given by

$$\theta_{Mg^{2+}} = \frac{1}{2}\left(1 - \frac{1}{\xi} - \theta_{Na^+}\right) \qquad (16)$$

where ξ is the linear charge density of A−RNA.[8] The total fraction ψ of counterions per polyion charge is obtained by the sum of $\theta_{Mg^{2+}}$ and the "screening counterions" per polyion charge. Because the average value of θ_{Na^+} is 0.55, we find that $\psi = 0.23$.

The variation of the observed equilibrium constant K_{obs} with magnesium ion concentration by holding Na^+ concentration fixed is shown in Figure 5. The slope of K_{obs} in the range 20−140 μM Mg^{2+} ions is

$$-\frac{\partial \log K_{obs}}{\partial \log[Mg^{2+}]} \approx 1.66 \qquad (17)$$

Equation 17 predicts that the number of ion pairs is approximately 7.2 since the total fraction of counterions per polyion charge is 0.23. This value for n_{eff} is consistent with the Hill coefficient determined by Kim et al.[18]

We briefly mention that there is another way to predict ψ that is not dependent on eq 16. This approach is based on exploiting three observations. First, the polyelectrolyte solution has univalent and divalent cations in addition to coion Cl^-. Second, a sum rule relates the preferential interacting coefficients of the univalent cation, univalent coion, and divalent cation.[7,30] Finally, Monte Carlo simulations on nucleic acid indicate that the preferential interaction coefficient of a univalent coion does not vary appreciably with magnesium ion concentration.[30]

Concluding Remarks. The near, far away, and intermediate regions that define the cloud of condensed ions, the Debye−Hückle counterions, and the coions, respectively, have some unique features. Imagine bringing a charge of valence z from infinity to a distance r from the polyion. If the region is a near region, then z univalent counterions are released from the condensed layer in agreement with eq 2. Analysis along the same lines as that in ref 28 indicates that if the region under consideration is a far away region, then the presence of the counterion has no effect on the number of condensed counterions on the RNA. In contrast, if the counterion is located in the intermediate region, then the number of counterions that are released into the bulk solution is $z(1 - \sigma)$, where σ is between zero and unity.[28] This result tends to suggest, in agreement with eq 15 and eq 17, that the counterions in a three-way A−RNA junction are located in the intermediate region. We anticipate that this prediction will stimulate new experiments.

It would be potentially fruitful to carry out Poisson−Boltzmann analysis of the salt−polyion preferential interaction coefficient of three-way RNA junction molecules in multivalent aqueous solution. Although this is a difficult problem, we have recently developed a new technique that allows us to place tight upper and lower bounds for the salt−polyion preferential interaction coefficient of linear DNA and RNA molecules of various linear charge densities by a variational solution of the cylindrical nonlinear Poisson−Boltzmann equation that is analytic, accurate, and valid from low to high concentration of univalent and multivalent cations.[31] We plan to generalize this work to three-way and four-way RNA and DNA junctions.

In summary, we have quantitatively described the ion atmosphere of three-armed symmetric Y-shaped and asymmetric y-shaped A−RNA junctions in multivalent aqueous solution within the framework of a polyelectrolyte model. The predictions for the slope of $\log(k_o/k_f)$ as a function of Na^+ and Mg^{2+} concentration, where k_o and k_f are the opening and folding rates of the three-helix junction molecule, respectively, are in reasonable agreement with the single-molecule FRET and FCS data of Kim et al.[18]

Acknowledgment. This work was supported by the National Science Foundation (U.M. and S.C.). One of us (U.M.) thanks M. Fenley and S. Mohanty for discussions.

Note Added after ASAP Publication. Figures 4 and 5 have been replaced with corrected values of the slopes in the insets. Corresponding corrections were made also in the figure captions and text. This paper was posted ASAP on 5/12/05. The corrected version was reposted on 6/15/05.

References and Notes

(1) Zarrinkar, P. P.; Williamson, J. R. *Nat. Struct. Biol*. **1996**, *3*, 432−438.
(2) Batey, R. T.; Williamson, J. R. *RNA* **1998**, *4*, 984−997.
(3) Wilson, T. J.; Lilley, D. M. J. *RNA* **2002**, *8*, 587−600.
(4) Uhlenbeck, O. C. *Nature (London)* **1987**, *328*, 596−600.
(5) Dahm, S. C.; Uhlenbeck, O. C. *Biochemistry* **1991**, *30*, 9864−9469.
(6) Bassi, G. S.; Murchie, A. I. H.; Lilley, D. M. J. *RNA* **1996**, *2*, 756−768.
(7) Anderson, C. F.; Record, M. T. *Annu. Rev. Phys. Chem*. **1995**, *46*, 657−700.
(8) Manning, G. S. *Q. Rev. Biophys*. **1978**, *11*, 179−246.
(9) (a) Conway, B. E. *Ionic Hydration in Chemistry and Biophysics*; Elsevier Scientific Publishing Co.: New York, 1981. (b) Misra, V. K.; Draper, D. E. *Biopolymers* **1998**, *48*, 113−135.
(10) Misra, V. K.; Honig, B. *Biochemistry* **1996**, *35*, 1115−1124.
(11) Shui, X.; McFail, I. L.; Hu, G.; Williams, L. *Biochemistry* **1998**, *37*, 8341−8355.
(12) Zana, R.; Tondre, B. *Biophys. Chem*. **1974**, *1*, 367−375.
(13) Cate, J. H.; Gooding, A. R.; Podell, E.; Zhou, K. H.; Golden, B. L.; Kundrot, C. E.; Cech, T. R.; Doudna, J. A. *Science* **1996**, *273*, 1678−1685.
(14) Pley, H. W.; Flaherty, K. M.; Mckay, D. B. *Nature (London)* **1994**, *372*, 68−74.
(15) Batey, R. T.; Williamson, J. R. *J. Mol. Biol*. **1996**, *261*, 550−567.
(16) Orr, J. W.; Hagerman, P. J.; Williamson, J. R. *J. Mol. Biol*. **1998**, *275*, 453−464.
(17) Nikulin, A.; Serganov, A.; Ennifar, E.; Tischenko, S.; Nevskaya, N.; Shepard, W.; Portier, C.; Garber, M.; Ehresmann, B.; Ehresmann, C. *Nat. Struct. Biol*. **2000**, *7*, 273−277.
(18) Kim, H. D.; Nienhaus, G. U.; Ha, T.; Orr, J. W.; Williamson, J. R.; Chu, S. *Proc. Natl. Acad. Sci. U.S.A.* **2002**, *96*, 9077−9082.
(19) Stryer, L.; Haugland, R. P. *Proc. Nat. Acad. Sci. U.S.A.* **1967**, *58*, 719−730.
(20) Selvin, P. R. *Methods Enzymol*. **1995**, *246*, 300−334.
(21) Rigler, R.; Mets, U.; Widengren, J.; Kask, P. *Eur. Biophys. J*. **1993**, *22*, 169−175.
(22) Maiti, S.; Haupts, U.; Webb, W. W. *Proc. Natl. Acad. Sci. U.S.A.* **1997**, *94*, 11753−11757.
(23) (a) Manning, G. S.; Mohanty, U. *Physica A* **1997**, *247*, 196−204. (b) Mohanty, U.; Ninham, B. W.; Oppenheim, I. *Proc. Nat. Acad. U.S.A.* **1996**, *93*, 4342−4344.
(24) Eisenberg, H. *Biological Macromolecules and Polyelectrolytes in Solution*; Clarendon: Oxford, 1976.
(25) Schurr, J. M.; Fujimoto, B. S. *Biophys. Chem*. **2002**, *101−102*, 425−445.
(26) Fenley, M. O.; Manning, G. S.; Marky, N. L.; Olson, W. K. *Biophys. Chem*. **1998**, *74*, 135−152.
(27) One can account for the compression or extension of the phosphate charges near the three-way junction by slightly varying the charge spacing around values consistent with structural information. However, this does not significantly change quantitative predictions of the model of such quantities as the number of associated counterions or the corresponding ionic free energy.
(28) Ray, J.; Manning, G. S. *Macromolecules* **1999**, *32*, 4588−4595.
(29) Record, M. T., Jr.; Lohman, T. M.; deHaseth, P. L. *J. Mol. Biol*. **1976**, *107*, 145−158.
(30) Anderson, C. F.; Record, M. T., Jr. *J. Phys. Chem*. **1993**, *97*, 7116−7126.
(31) Taubes, C. H.; Mohanty, U.; Chu, S. Unpublished, 2004.